Journal of Solid State Electrochemistry (2018) 22:3965–3975
https://doi.org/10.1007/s10008-018-4098-5

ORIGINAL PAPER

Regeneration of expanded graphite electrodes by joined electrochemical and ozone treatment in liquid phase

A. Bachar[1] · B. Gurzęda[1] · J. Zembrzuska[1] · M. Nocuń[2] · P. Krawczyk[1]

Received: 22 March 2018 / Revised: 23 August 2018 / Accepted: 8 September 2018 / Published online: 21 September 2018

Abstract

The researches presented in this work were devoted to electrochemico-chemical regeneration of exhausted electrode made of expanded graphite (EG). The aimed process was conducted by electrochemical treatment and ozone flow performed together in wet environment. EG was covered with insoluble products of incomplete oxidation of phenol formed during cyclic voltammetry measurement. The same electrochemical technique was applied for evaluation of regeneration efficiency. To understand the process of EG regeneration, the electrode was characterized by calculating of BET surface, FTIR and XPS analysis. Moreover, SEM images of the investigated samples were also done. Obtained results have showed the success of regeneration treatment, which led to significant enhancement of electrode activity compared to original EG. The present work also revealed that the mechanism of phenol electrooxidation is changed after the regeneration treatment of electrode material. This effect is probably caused by the modification of chemical composition of EG surface due to its interactions with OH radicals intensively generated during the process of regeneration.

Keywords Expanded graphite · Phenol electrooxidation · Ozone treatment · Electrode regeneration

Introduction

The development of modern world is connected with the production of more and more pollution, which requires working out new methods to cope with them. One of the most dangerous and toxic substance is phenol. It can be neutralized to non-toxic carbon dioxide CO_2 and water H_2O by biodegradation [1–3], chemical [4], electrochemical [5–7], and photochemical oxidation. Electrochemical methods are widely used because they can be highly controllable thus enabling the formation of product of a desired properties. There are many factors, such as type of electrode material, electrode mass, pH and type of electrolyte, temperature, initial concentration of phenol, which have influence on the course of phenol electrooxidation. Variety of electrodes were used in the process of electrochemical oxidation of phenol, for example platinum [8], IrO_2 [9], RuO_2 [10], SnO_2 [11], and PbO_2 [12]. Among the electrodes successfully used for phenol oxidation are also carbon electrodes made of graphite [13], expanded graphite [7, 14], active carbon [15], and boron-doped diamond [16].

Regarding the electrochemical oxidation of phenolic compounds it should be mentioned one major problem. In some cases, phenol is oxidized only partially and the unwanted by-products are formed. They can react with each other thus creating an insoluble layer of oligomeric products on the surface of electrode. That effect is strongly undesirable because the oligomer layer is electrochemically inactive and lowers the current flow, which means that the electrode becomes useless from the practical point of view. The above mentioned problem is observed for various types of electrodes [17–20]. That undesired behavior also occurs for the graphite-based electrodes [7, 14, 21]. On such a case, there is a need to regenerate the spent electrodes enabling its reuse. Depending on the type of electrode, the process of regeneration can be realized by thermal [15, 22, 23], chemical [24], and electrochemical treatment [7, 14, 21, 25, 26].

Two main criteria are used for estimation of regeneration efficiency. One of them is based on the degree of recovered

✉ P. Krawczyk
piotr.krawczyk@put.poznan.pl

[1] Institute of Chemistry and Technical Electrochemistry, Poznan University of Technology, ul. Berdychowo 4, 60-965 Poznań, Poland

[2] Faculty of Materials Science and Ceramics, AGH University of Science and Technology, al. Mickiewicza 30, 30-059 Kraków, Poland

electrochemical activity, whereas the latter one is associated with the mass loss of regenerated material due to aggressive regeneration treatment. Our previous works have shown that owing to the electrochemical methods, it is possible to recover and even significantly improve the initial activity of graphitic electrodes without damage to its structure [14, 25].

Ozone is a highly reactive molecule. Hence, in wastewater treatment, it can be used as disinfectant or biocide, oxidant to remove organic pollutants and as well as a pre- or post-treatment agent in other processes, such as flocculation or sedimentation [27]. What is more, ozone is commonly used for creation as well as modification of active surface of carbon materials [24, 28, 29]. In each case, ozonation increases oxidation degree, because of effective formation of functional groups containing oxygen. Most of the processes are held in gas phase, but there are examples of ozone treatment which were realized in liquid environment (acidic, basic, or neutral) [30, 31]. Among the carbon used for ozone treatment were active carbons, carbon black, carbon fibers, and graphitic materials [28, 29].

Ozone can be also used for regeneration of spent electrodes. In this case, process is usually conducted by exposing the electrode to ozone flow under different conditions, such as treatment duration, ozone concentration, environment, temperature, and supporting treatment like ultrasounds or UV radiation. The crucial factor seems to be the time of ozonation; however at some point, the longer time gives no more better result. Process of ozone regeneration is performed in gas phase, but liquid environment like water, bases, or acid solutions is also used [32, 33]. Despite the conditions used, in many cases, the mechanism of ozone regeneration is similar. Ozone plays a role of oxidant which reacts with substance occupied the electrode surface. When liquid solution is used, ozone can be the oxidant itself or be a factor to produce oxidants for indirect regeneration.

The purpose of this paper was to examine the process of regeneration of expanded graphite being exhausted with oligomeric products of phenol oxidation. The considered regeneration comprises of interactions between EG/oligomer and OH radicals intensively created during joined ozone and electrochemical oxidation processes.

Experimental

Preparation of expanded graphite

Expanded graphite (EG) was obtained by thermal exfoliation of graphite intercalation compound with sulfuric acid (H_2SO_4-GIC), which was synthesized in process of anodic oxidation of flaky graphite in 18 M H_2SO_4 [7].

Preparation of electrode and electrochemical measurements

EG electrode was subjected to cyclic voltammetry measurements realized with three-electrode system. Process of electrochemical oxidation of phenol was performed with a scan rate 0.1 mVs^{-1} in the potential range from the rest potential of electrode (E_R) to 0.8 V. Electrolyte was composed of 0.5 M aqueous solution of KOH containing 0.1 M phenol. The reference electrode was Hg/HgO/0.5 M KOH (0.117 V vs. NHE), whereas graphite rod (5 mm in diameter) served as a counter electrode. EG being a powder type electrode was put around a graphite rod (5 mm in diameter) in a pocket made of porous non-active material. Graphite rod was playing a role of current collector. In each case, the mass of working electrode was equal to 15 mg. After the process, spent electrode (EG/oligomer) was taken out from the cell, rinsed with distilled water and left to dry on air. All electrochemical measurements were conducted using AUTOLAB potentiostat-galvanostat (model PGSTAT 30). Process of EG/oligomer regeneration was carried out for 1 h in 6 M KOH using potentiostatic method with constant potential 1.3 V. The rest part of electrochemical system was the same as that used for phenol oxidation. The turbulent flow of ozone with rate of 0.9 dm^3/min was introduced by hose. Ozone was gathered from ozone generator supplied with air. In order to estimate the efficiency of regeneration process, the regenerated EG was used as a working electrode for phenol electrooxidation performed under the same conditions as previously described. The comparison of current charges associated with peak of phenol oxidation for regenerated sample with that noted for original EG was a source of information on efficiency of restoration of electrode activity. Samples gathered after 3 cycles of voltammetric oxidation of phenol and regeneration were denoted as EG-3Ph and EG-3Ph reg, respectively.

Properties of EG electrode before and after regeneration

Taking into account, the properties of EG three following aspects were studied: morphological properties, chemical composition of surface, and the development of specific surface area. The first aspect was examined by scanning electron microscopy (SEM) (S-3400N, Hitachi microscope) using a voltage acceleration of electron beam equal to 15 keV. Information on chemical composition was acquired from the FTIR and XPS spectroscopy investigations. FTIR measurements were conducted on JASCO model FT/IR-6700 spectrometer, using KBr technique, whereas the XPS measurement was performed with VSW spectrometer equipped with hemispherical analyzer. The changes within the specific surface area of EG due to its regeneration were determined from the N_2 adsorption isotherms measured at 77 K with ASAP 2010 apparatus.

Concentration of OH radicals

In order to propose a mechanism of EG-3Ph regeneration, an analysis of OH radicals concentration in the electrolyte was done. The preparation process was based on Peralta work [34] but with some modifications. The samples used for OH radicals determination were the following solutions: (1) 6 M KOH acquired after electrochemical regeneration of EG-3Ph, (2) 6 M KOH gathered after electrochemical-chemical regeneration of EG-3Ph, and (3) ozonated 6 M KOH.

After regeneration and/or ozonation to the solution was added salicylic acid (2 mL) in amount equal to KOH molarity. Salicylic acid reacts with OH radicals yielding 2,5-DHBA (dihydroxybenzoic acid) and 2,3-DHBA (dihydroxybenzoic acid). Another product of the abovementioned reaction could be catechol, but in this case, it was not detected in the investigated solutions.

Analytical system

The concentrations of 2,5-DHBA and 2,3-DHBA in samples were determined using liquid chromatography (UltiMate 3000, Dionex, Sunnywale, CA, USA) coupled with a mass spectrometer (API 4000 QTRAP, AB Sciex, Foster City, CA, USA). Acids were separated on C18 column (Hypersil Gold C18 RP, 100 × 2.1 mm × 1.9 μm, Thermo Scientific, USA) with an isocratic mobile phase consisting of acetonitrile and water with 0.1% formic acid (1:1, acetonitrile–water, *v*/*v*). The flow rate was 0.2 mL/min, the injection volume was 10 μL. The column was kept at 35 °C. The mass spectrometer was operated in turbo ion spray in the negative ion mode. All acids were detected using the following settings for the ion source and mass spectrometer: curtain gas 10 psi, nebulizer gas 40 psi, auxiliary gas 40 psi, temperature 450 °C, ion spray voltage − 4500 V. Quantification was performed by multiple reaction monitoring (MRM). The mass transition used for 2,5-DHBA was *m*/*z* 153 → 109 (with a declustering potential − 55 V and collision energy − 30 V) and for 2,3-DHBA was *m*/*z* 153 → 109 (with a declustering potential − 35 V and collision energy − 22 V).

Standard solutions and sample preparation

A stock standard solutions for each compound was prepared in acetonitrile. The solution was stored at 4 °C.

All samples were filtered and diluted. The method of multiple standard additions was used for evaluation of each compounds concentration. The sample and sample spiked standard mixture at three different concentrations (0.0005; 0.001 and 0.0025 μg/mL) was determined by LC-MS/MS. Standard spikes were added to the sample directly before the analysis. An example of the standard addition is shown in Fig. 1.

Results and discussion

Electrochemical oxidation of phenol

Cyclic voltammograms recorded during electrochemical oxidation of 0.1 M phenol dissolved in 0.5 M KOH at electrode made of expanded graphite are presented in Fig. 2. Phenol electrooxidation is depicted as a huge anodic peak recorded during the forwarded scanning. During the first cycle, maximum of this peak appears at around 0.55 V but for the next cycles, its location is shifted towards the lower potentials (0.48 V). The significant decrease in intensity of anodic peak after the first cycle is connected with the formation of insoluble layer of oligomer being product of the incomplete oxidation of phenol [18–20]. For the first cycle charge of anodic peak is equal to 13.99 C, whereas for the second and third cycle reached 8.87 C and 8.68 C, respectively (Table 1). The observed deterioration in electrochemical activity of EG electrode due to its blocking by passive oligomer justifies the necessity of its regeneration. Hence, our further investigations were focused on the process of electrochemico-chemical regeneration of spent EG electrode. The conducted regeneration was based on the anodic oxidation of EG supported by the gaseous ozone passed through the electrolyte in which the regeneration was performed.

Figure 3 presents cyclic voltammograms recorded during phenol oxidation at electrode made of EG underwent regeneration. The shape of the obtained curves is similar to that shown for original EG (Fig. 2). One can also observe a huge anodic peak responsible for the phenol oxidation. It is located at the potential of about 0.42 V. For the second and third cycles, the mentioned peak can be seen at lower potential 0.4 V. It is worth to note that the location of phenol oxidation peak is slightly shifted towards the less positive potentials as compared to the not regenerated electrode (Fig. 2). For the regenerated electrode during the first cycle, charge of anodic peak was equal to 45.04 C, whereas for the second one only 21.99 C (see Table 1). It can be observed that by comparing to the original EG activity of regenerated electrode is doubled and even more (see Fig. 4). Our previous papers [18, 20] have already mentioned about that phenomena but in this case, the observed rise is significantly larger.

By comparing the location as well as intensity of the considered peak, it can be stated that the mechanism of phenol oxidation significantly differs depending on the applied electrode. For the regenerated electrode (see Fig. 3), process of phenol oxidation starts at lower potential compared to the untreated electrode (see Fig. 2). Maximum of phenol oxidation peak for regenerated EG is also shifted towards the less positive potentials. Additionally, the intensity as well as current charge associated with the peak of phenol oxidation for regenerated electrode is markedly higher as compared to the original electrode. The abovementioned observations indicate

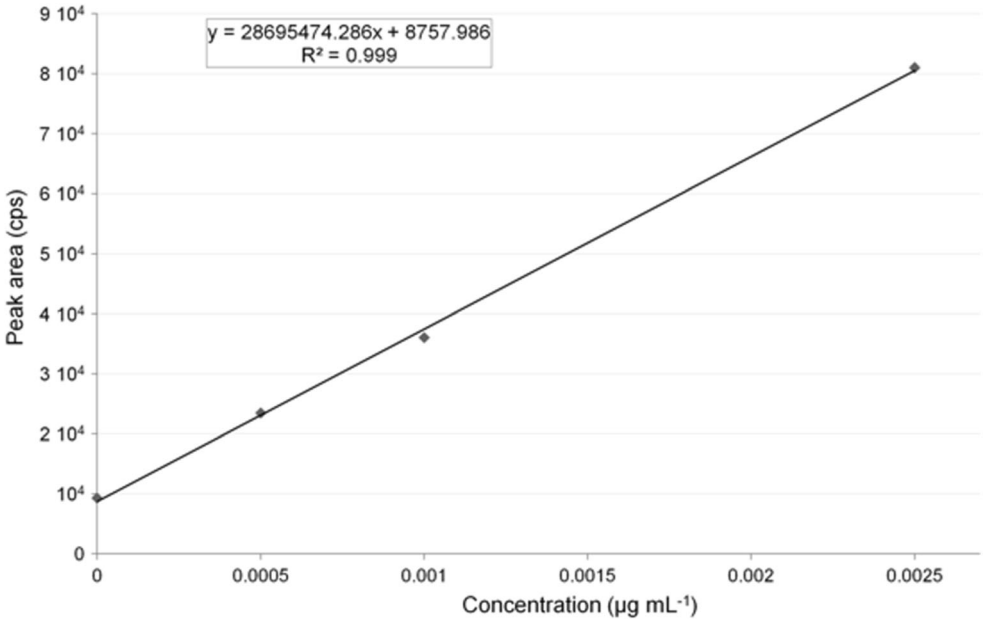

Fig. 1 Multiple standard curve of 2,5-DHBA for sample of electrolyte after electrochemical-chemical regeneration of expanded graphite covered in phenol during 3 cycles of electrooxidation

that the electrochemical oxidation realized together with ozone treatment of spent EG electrode not only recover but significantly improves its electrochemical activity. The differences in the course of CVs suggest that the regeneration treatment considerably modify electrode material by making it much more active and suitable for phenol oxidation.

In order to understand the origin of activity increment due to regeneration treatment, the additional investigations were performed. The sample of original EG being free of oligomer underwent electrochemical oxidation with accompaniment of ozone treatment under conditions employed for EG/oligomer regeneration. Such modified EG was used as a working electrode during the electrochemical oxidation of phenol and CVs recorded in 0.1 M phenol dissolved in 0.5 M KOH are shown in Fig. 5. As can be seen, the course of voltammetric curves

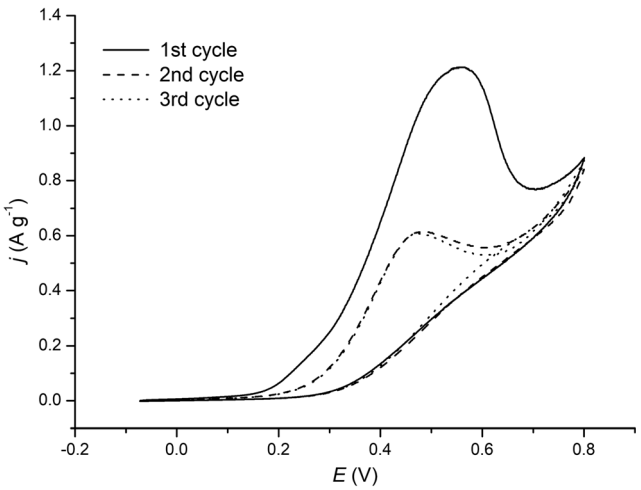

Fig. 2 Cyclic voltammograms for original EG recorded in 0.1 M phenol in 0.5 M KOH

significantly differs compared to that observed for original (Fig. 2) as well as for regenerated EG (Fig. 3). The most pronounced differences are related with the intensity and location of anodic peak associated with the reaction of phenol oxidation. It indicates that the oxidative treatment of EG resulted in increment of its electrochemical activity towards the phenol electrooxidation. Anodic charge associated with phenol oxidation on modified EG (EG-KOH-O_3) is over twice higher than that noted for original EG (Table 1). It is worth to note that this relation is observed not only for the first cycle but for all presented. On the other hand, it should be emphasized that the activity level of modified EG is over 1.5 times lower as compared to that observed for the first cycle for regenerated electrode (EG-3Ph reg) (Fig. 3). By comparing the successive cycles, it is clear that for both cases, the electrochemical activity appear on very closed level. One of the possible explanation of this behavior may be associated with the modification of oligomer occupied the surface of EG. Due to regeneration treatment oligomeric film considerably changes its properties thus improving the electrochemical activity of EG electrode.

The supposed changes in oligomer behavior resulting improvement of electrochemical activity of regenerated

Table 1 Values of anodic charge calculated for the investigated samples on the basis of cyclic voltammetry measurements

	EG [C]	EG-3Ph reg [C]	EG-KOH-O_3 [C]
Cycle 1	13.99	45.04	29.52
Cycle 2	8.87	21.99	20.85
Cycle 3	8.68	18.21	17.94
Cycle 1–3	31.54	85.24	68.31

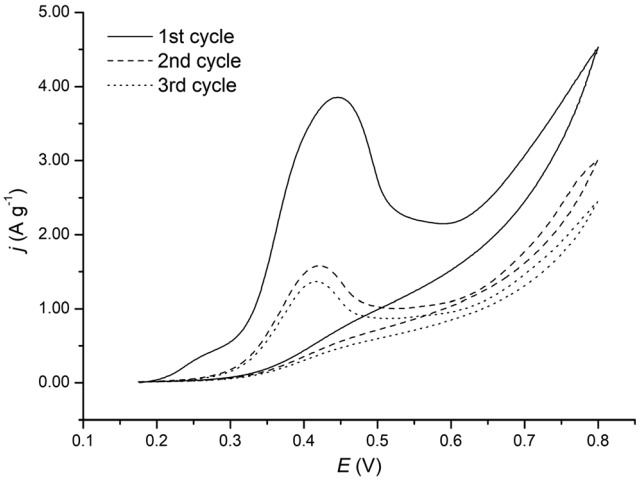

Fig. 3 Cyclic voltammograms recorded in 0.1 M phenol in 0.5 M KOH for EG after its regeneration (EG-3Ph reg)

electrode towards the process of phenol oxidation most likely are associated with the modification of EG especially chemical composition of its active surface. Hence, this issue becomes the goals of our further investigations.

XPS measurements

Table 2 contains information on surface content of EG, spent EG, and regenerated EG calculated on the basis of XPS measurements. It can be easily observed that due to phenol oxidation the amount of oxygen on EG surface increases. The oligomer layer which is formed on EG surface during phenol electrooxidation involves oxygen containing bonds. From the O1s spectra shown in Fig. 6 it can be seen that the regeneration reduces total oxygen content but it is still higher than that noted for original EG. It proves that despite some changes in chemical composition, the persisting oligomer still involved some oxygen bonds. Taking into account the particular composition of surface of the regenerated sample, an increment in concentration of O=C bonds probably pertaining to ketones, lactones, or carboxylic is easily seen from the O1s spectrum. On the other hand, the amount of O−C bonds of phenolic or/and etheric group decreases due to regeneration treatment. It means that O−C bonds being the main component of oligomer film generated on EG surface during the phenol oxidation disappear or/and are transformed into the C=O during the regeneration treatment. These observations well coincide with the results gathered from the C1s spectra seen in Fig. 7. Peak B on spectrum for EG-3Ph reg probably arises from the presence of C−O bonds (phenolic, ether) but it can be also associated with K−O bond, which could be built-in during the regeneration performed in KOH containing electrolyte. Taking into account its participation in a whole C content, it is seen that the concentration of C−O and/or K−OH bonds grow up during phenol oxidation and simultaneously slightly decreases after the regeneration treatment. It should be noted that the most pronounced influence of electrolyte on the composition of electrode surface is associated with the presence of peak at 293.6 eV. This signal is likely associated with the potassium ions being incorporated into the oligomer chain during the regeneration treatment. The O1s/C1s ratio calculated from the concentration of C−O bond (peak C) on O1s spectrum and peak B on C1s spectrum for EG-3Ph reg reached 0.28 while for EG sample after phenol oxidation (EG-3Ph) is equal to 0.12. It indicates that for regenerated sample, the higher participation in peak B on C1s spectrum might have K−O bond than C−O. Peak C on the deconvoluted spectra C1s (Fig. 7) represents double bonds between C and O of quinone and carbonyl functionalities. C1s spectrum for EG after its regeneration treatment (EG-3Ph reg) involves two new peaks as compared to the spectra

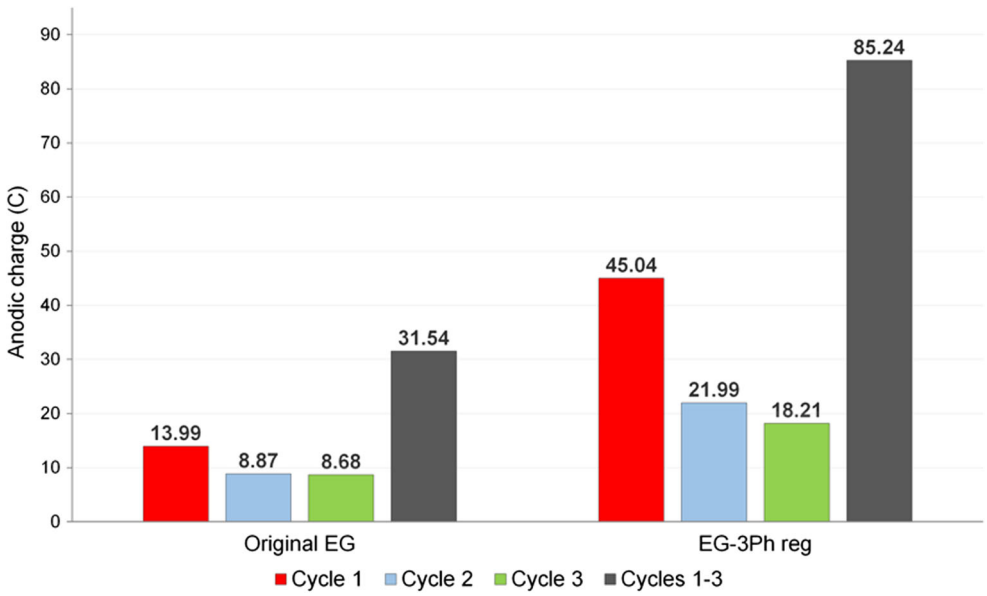

Fig. 4 Comparison of anodic charges recorded during electrochemical phenol oxidation for original and regenerated EG electrodes

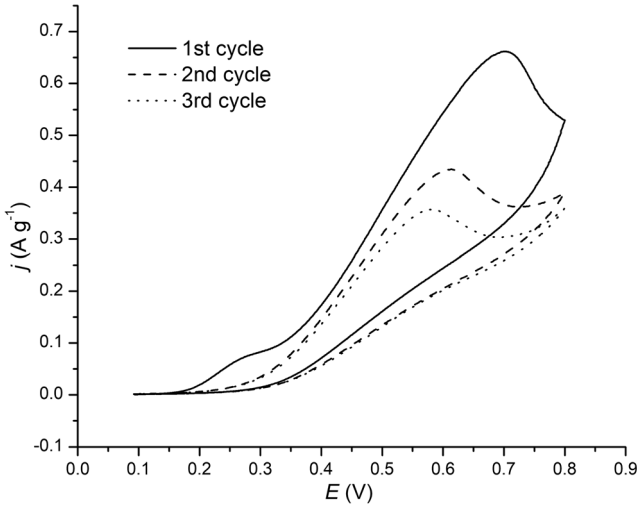

Fig. 5 Cyclic voltammograms for original EG underwent oxidative treatment (electrochemical and ozone) recorded in 0.1 M phenol in 0.5 M KOH

recorded for original EG and EG after 3 cycles of phenol electrooxidation (EG-3Ph). The former one (peak D) can be ascribed to the C=O bonds pertaining to carboxylic groups, whereas the latter peak (peak F) reveals the presence of K containing bonds. The latter effect most likely arises from the interactions between the electrolyte and oligomer covering the EG surface. It should be also noted that the regeneration treatment of EG/oligomer composite decreases signals associated with the graphitic skeleton (peaks A and E).

From the XPS results, it is clear that wet ozone treatment performed together with electrochemical oxidation change the chemical surface of regenerated EG. Some of transformations within the surface oxide bonds are accompanied by the formation of a new one composed of potassium ions. The last statement is proved by two new peaks appearing at 293.6 eV which show building-in of the potassium ions.

FTIR measurements

Figure 8 displays FTIR spectra recorded for the investigated samples, whereas Table 3 involves the assignment of the bands seen on the presented infrared spectra. The comparison of FTIR spectra for original EG, EG after phenol oxidation, and EG after regeneration treatment allow to evolve the crucial differences in chemical composition of their surfaces. It seems that the most valuable information can be gained from the region of 1000–2000 cm^{-1}, therefore only this part of whole spectrum is shown in Fig. 8. Bonds seen at wavenumber of 1219, 1292, and 1398 cm^{-1} are connected with the graphite matrix itself without functionalities. What is interesting, bond at 1219 cm^{-1} assigned to the ring vibrations is observed for samples EG and EG-3Ph reg but not for EG-3Ph. It well correlates with the appearance of E peak on XPS spectra of C1 region (Fig. 7). Most of the presented bands being associated with the oxygen containing surface functionalities are shown between 1400 and 2000 cm^{-1}. It can be easily perceived that more of them were created during regeneration treatment of EG. From the data shown in Table 3, it is clear that the regeneration increases the concentration of C = O and COO bonds which also agrees with the XPS results. Bands at

Table 2 XPS results: surface composition of original EG, EG after 3 cycles of phenol oxidation (EG-3Ph), and after regeneration treatment (EG-3Ph reg)

Spectrum	Peak/ sample	EG			EG-3Ph			EG-3Ph reg			The assignment of XPS peaks
		(eV)	(at.%)	Total content (at.%)	(eV)	(at.%)	Total content (at.%)	(eV)	(at.%)	Total content (at.%)	
O1s	A	530.4	0.09	3.35	530.6	0.94	13.05	531.3	2.09	9.26	O=C (ketone, lactone, carboxylic) [30, 31]
	B	532.1	0.80		531.6	3.54		532.7	3.57		O=C (carbonyl) [32]
	C	533.4	1.16		533.3	7.83		534.1	2.89		O-C (phenolic, etheric) [27, 31]
	D	534.7	1.30		534.8	0.86		535.7	0.71		Chemisorbed oxygen [33]
C1s	A	284.6	61.12	95.65	284.6	47.27	86.95	284.6	35.64	90.74	C (graphitic carbon) [27, 31–33, 35]
	B	285.9	20.70		285.7	27.98		285.5	23.24		C-O (phenolic, etheric) [31, 36] *or* K-O [37]
	C	287.3	8,2		287.4	8,23		286.7	15.50		> C = O (quinone, carbonyl) [31, 32]
	D							288.2	7.41		C = O (carboxyl) [31, 32]
	E	290.7	6.56		289.2	3.47		290.1	3.09		π-π transition in aromatic systems [27, 31–33, 35]
	F							293.6	5.86		C-KOH [37]

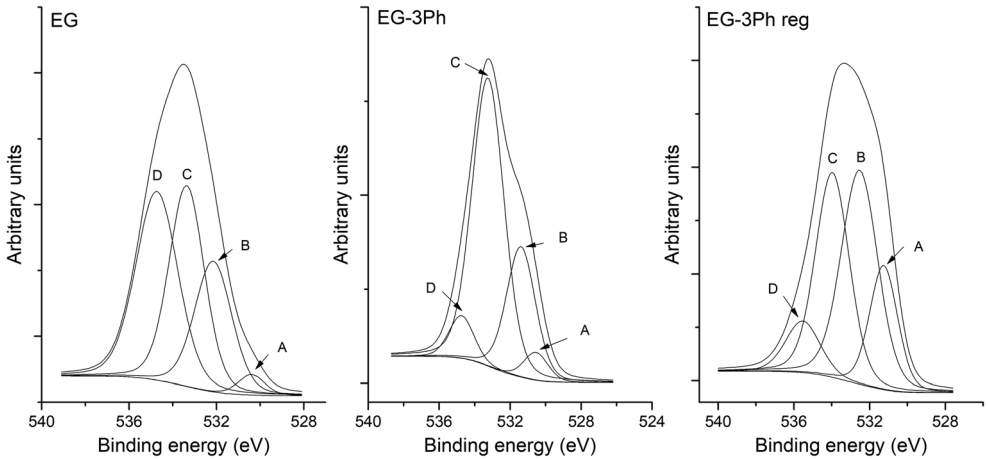

Fig. 6 XPS spectra of O1s region

wavenumber of 1537, 1555, 1663, 1692, and 1775 cm^{-1} can be assigned to the C = O bonds in carboxylic acids, ketones, and quinones, respectively. The appearance of the abovementioned bonds is also revealed from C1s spectrum of XPS analysis (see Fig. 7). The bands at 1692 and 1752 cm^{-1} are ascribed to C = O stretch vibrations in ketones and lactones. The appearance of these groups is confirmed on XPS spectrum of a O1s region recorded for the regeneration sample (see Fig. 6) (Table 3).

Summarizing the obtained results, it can be pointed out that the phenol oxidation significantly changes the surface of the electrode by formation of oligomeric structures but subsequently performed regeneration treatment involved simultaneous electrochemical and ozone oxidation in turn modify the surface of electrode thus allowing its reuse.

BET measurements and SEM observations

BET analysis reveals information on changes in EG structure due to its regeneration treatment. The started EG exhibits BET surface area of 30.5 $m^2\ g^{-1}$ whereas the BET surface of EG after 3 cycles of phenol electrooxidation falls down to 7.1 $m^2\ g^{-1}$. The huge decrease in specific surface area due to phenol oxidation proves the presence of passive oligomer layer. That nonconductive layer is responsible for the worsening of electrochemical activity observed on voltammogram during the second cycle of cyclic voltammetry oxidation of phenol. After regeneration treatment, the specific surface area in turn rises to 21.8 $m^2\ g^{-1}$ but it does not reach the original development area value. It might be explained by the fact that persisted oligomer layer still occupy the EG surface. It is possible that due to regeneration treatment, the oligomer layer becomes much more porous as compared to that gathered after phenol oxidation. In some part, the abovementioned suppositions are confirmed by the SEM images for the EG before and after regeneration treatment (Fig. 9). In order to understand the impacts of electrochemical oxidation and subsequent regeneration treatment on morphology of EG, the SEM image of original EG was added (Fig. 9a). SEM micrograph obtained for EG after its use in process of phenol electrooxidation (Fig. 9b) undoubtedly proves the appearance of oligomeric film. Almost whole surface of EG is coated with a thin layer of oligomer. Only central part of flake seems to be

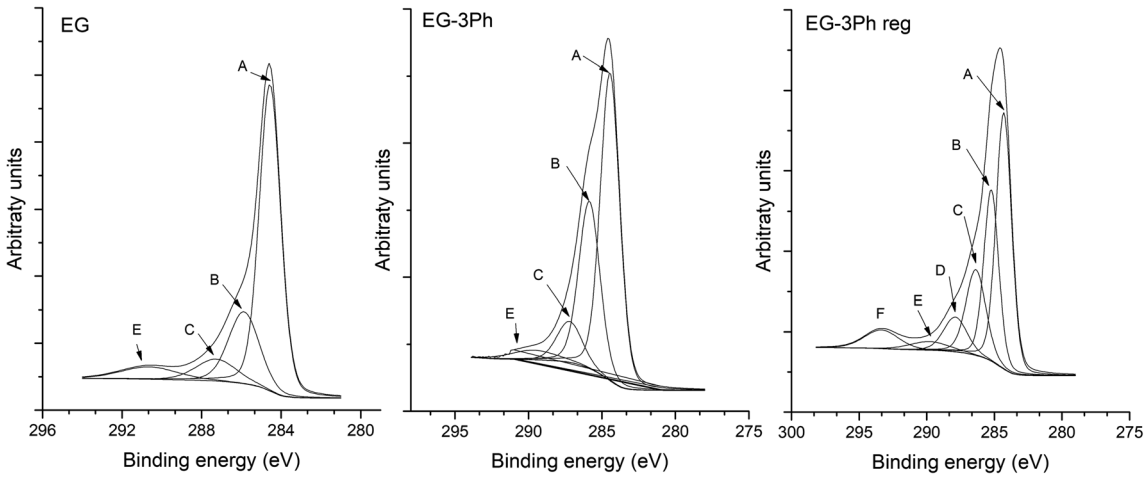

Fig. 7 XPS spectra of C1s region

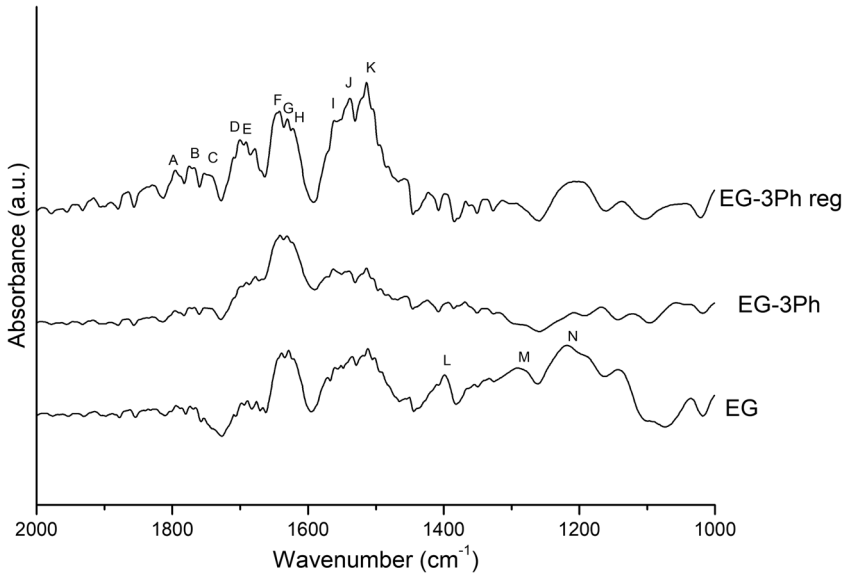

Fig. 8 FTIR spectra recorded for original EG, EG after 3 cycles of phenol electrooxidation (EG-3Ph) and ozone wet treated (EG-3Ph reg)

uncovered depicting a characteristic accordion like structure of exfoliated graphite. After the regeneration treatment some part of oligomer are removed from the graphite surface. However, some residuals of oligomer still occupied the EG surface which is illustrated by the curled up and irregular elements seen in the middle of the SEM image shown in Fig. 9c. SEM image of regenerated EG recorded under higher magnitude also revealed the increased concentration of edges as well as surface defects (see Fig. 9d). Due to regeneration chemical composition of EG significantly changes by some transformations and in the functionalities originally present on EG sample as well as formation of a new one mainly by incorporation of potassium ions. As can be seen from the SEM images, the regeneration treatment involved electrochemical oxidation and chemical treatment by agents formed by ozone interactions with KOH electrolyte also results in increased concentration of surface defects as well as edges. These elements may play a role of active centers in which the oxygen functionalities can be build.

OH radicals analysis

It is assumed that OH radicals play a main role during the regeneration of spent EG electrodes.

The abovementioned radicals are formed during the both electrochemical as well ozone regeneration. In order to confirm our hypothesis the concentration of OH radicals in

Table 3 The assignment of the FTIR bands shown in Fig. 8

No.	Peak (cm^{-1})		Surface group	Assignment	Reference
	This work	Reference			
A	1796	1740–1800	C = O	Stretch in saturated aliphatic carboxylic acids	[38, 42]
B	1775	~1775	C = O	Stretch in phenyl acetates	[38, 42]
C	1752	1740–1765	C = O	Stretch in lactones	[38, 42]
D	1699	1698	COO	Stretch of COO	[38, 42]
E	1692	1694	C = O	Stretch in aliphatic ketones	[39, 43]
F	1663	1540–1700	C = O	Quinone or conjucted ketone	[38, 45]
G	1630	1629	C = C	Stretch of C = C in aromatic rings	[41, 44]
H	1621	1580–1660	C = C	Conjugated with C = C or C = O	[38, 45]
I	1555	1558	C = O	Stretch of C = O	[41, 44]
J	1537	1530–1610	COO	Asymmetric in aromatic acid salts	[38, 42]
K	1513	1510	C = C	Highly red-shifted C = C	[40, 45]
L	1398	1360–1430	CH = CH	cis	[42]
M	1292	1270–1350	CH_3	symmetric	[42]
N	1219	1180–1220	Ar	Ring vibrations	[42]

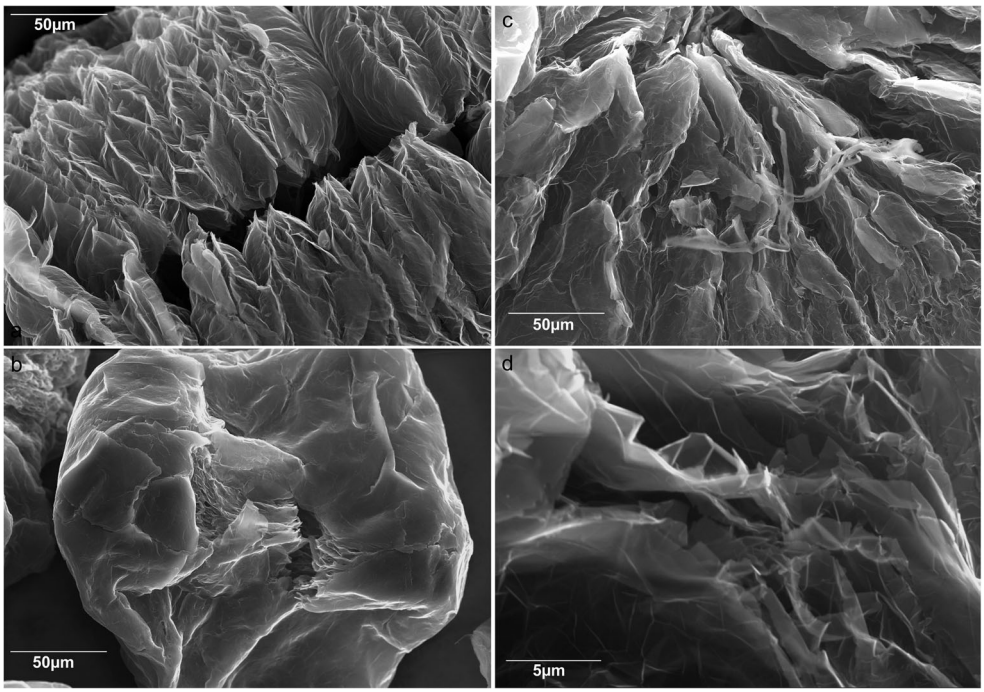

Fig. 9 SEM micrographs of original EG (**a**), EG after 3 cycles of phenol electrooxidation (EG-3Ph) (**b**), and regenerated EG (EG-3Ph reg) (**c**, **d**)

electrolyte after regeneration treatment under different conditions was performed. The compounds were determined in a non-spiked and spiked at three levels: 0.0005, 0.001, and 0.0025 μg/mL. Determination was performed in accordance with details given in "Analytical system". The obtained results are shown in Table 4. As can be seen, only 2,5-DHBA were identified in the all samples. The highest concentrations were determined for sample of 6 M KOH solution beforehand underwent ozonation (1112.10 μg/mL), whereas the lowest were observed for sample of electrolyte of 6 M KOH after electrochemical-chemical regeneration of EG-3Ph conducted in ozone flow (486.56 μg/mL). 2,3-DHBA was identified only in the case of ozonated 6 M KOH solution (213.20 μg/mL).

These results indicate that both during electrochemical regeneration itself and electrochemical regeneration supported by ozone, OH radicals are formed. At the beginning, it may be thought that ozonation limits the number of created radicals. Therefore, a solution of 6 M KOH without the sample of exhausted expanded grapite, was ozonated to check it. Surprisingly, it seems that process of ozonation creates incredible number of OH radicals. It indicates that during the process of joined regeneration of EG-3Ph, significantly higher amount of OH radicals is consumed to oxidize oligomer layer on electrode surface compared to the process realized only by electrochemical mode.

Conclusions

The researches have shown that inactive EG electrode coated with oligomeric film being the product of incomplete phenol electrooxidation can be successfully regenerated using joined electrochemical and ozone wet treatment not only to give back the previous activity but also to improve it almost double. The results of XPS and FTIR analyses revealed changes in chemical composition of EG surface due to regeneration treatment. Compared to the initial EG, it can be observed lowering the concentration of graphitic carbon which is accompanied by the modification of oxygen containing surface functionalities. The most pronounced result of regeneration treatment is associated with the increment in concentration of C=O bonds pertaining to carbonyl as well as carboxyl groups. The mentioned investigations also showed that the potassium ions from the solution are built-in on oligomer covering the surface

Table 4 Concentration [μg/mL] of 2,5-DHBA and 2,3-DHBA in samples of electrolytes used

Sample of electrolyte	2,5-DHBA	2,3-DHBA
6 M KOH after electrochemical regeneration of EG-3Ph	844.83	–
6 M KOH after electrochemical-chemical regeneration with ozone flow of EG-3Ph	486.56	–
6 M KOH after ozonation	1112.10	213.20

of EG electrode. The study of electrolyte composition has shown that the quantity of OH radicals being created during the regeneration treatment changes. Significantly higher concentration of OH radicals is reached during the joined regeneration evidencing the highest efficiency of chemical interactions between OH radicals and electrode surface. Taking into account, all results, the modification of surface oxygen groups, and the presence of K ions being incorporated into the oligomer chain may be the key factor which improves the activity of EG electrode during electrooxidation of phenol.

Acknowledgements This work was financially supported by the National Science Centre of Poland (2015/17/B/ST8/00371).

References

1. Wang Y, Chen H, Liu YX, Ren RP, Lv YK (2016) An adsorption-release-biodegradation system for simultaneous biodegradation of phenol and ammonium in phenol-rich wastewater. Bioresour Technol 211:711–719
2. Banerjeea A, Ghoshal AK (2016) Biodegradation of phenol by calcium-alginate immobilized Bacillus cereus in a packed bed reactor and determination of the mass transfer correlation. J Environ Chem Eng 4(2):1523–1529
3. Acikgoza E, Ozcan B (2016) Phenol biodegradation by halophilic archaea. Int Biodeterior Biodegrad 107:140–146
4. Danov SM, Orekhov SV, Fedosov AE, Fedosova ME, Shishkin AI (2015) Patterns of phenol oxidation process with an aqueous solution of hydrogen peroxide. Khim Tekhnol 16(3):157–162
5. Chen G (2004) Electrochemical technologies in wastewater treatment. Sep Purif Technol 38(1):11–41
6. Martinez-Huitle CA, Ferro S (2006) Electrochemical oxidation of organic pollutant for the wastewater treatment: direct and indirect processes. Chem Soc Rev 35(12):1324–1340
7. Skowroński JM, Krawczyk P (2004) Electrooxidation of phenol at exfoliated graphite electrode in alkaline solution. J Solid State Electrochem 8(6):442–447
8. Vlyssides A, Papaioannou D, Lozidoy M, Karlis P, Zorpas A (2000) Testing an electrochemical method for treatment of textile dye wastewater. Waste Manag 20(7):569–574
9. Chatzisymeon E, Fierro S, Karafyllis I, Mantzavinos D, Kalogerakis N, Kastaounis A (2010) Anodic oxidation of phenol on Ti/IrO_2 electrode: experimental studies. Catal Today 151(1-2): 185–189
10. Tran LH, Drogui P, Mercier G, Blais JF (2009) Electrochemical degradation of polycyclic aromatic hydrocarbons in creosote solution using ruthenium oxide on titanium expanded mesh anode. J Hazar Mater 164(2-3):1118–1129
11. Hu F, Cui X, Chenz W (2010) Pulse electro-codeposition of Ti/SnO_2-Sb_2O_4-CNT electrode for phenol oxidation. Electrochem Solid-State Lett 13(9):F20–F23
12. Samet Y, Agengui L, Abdelhedi R (2010) Anodic oxidation of chlorpyrifos in aqueous solution at lead dioxide electrodes. J Electroanal Chem 650(1):152–158
13. Chen JL, Chiou GC, Wu CC (2010) Electrochemical oxidation of 4-chlorophenol with granular graphite electrodes. Desalination 264(1-2):92–96
14. Skowroński JM, Krawczyk P (2007) Improved electrooxidation of phenol at exfoliated graphite electrode. J Solid State Electrochem 11:223–230
15. Shiter GE, Shindler Y, Matattov-Meytal Y, Grader GS, Sheintuch M (2002) Thermal behavior of the phenol-Pd-ACC system. Carbon 40(14):2547–2557
16. Elaoud SC, Panizza M, Cerisola G, Mhiri T (2011) Electrochemical degradation of sinapinic acid on BDD electrode. Desalination 272(1-3):148–153
17. Gottrell M, Kirk DW (1992) A Fourier transformation infrared spectroscopy study of the passive film produced during aqueous acidic phenol electro-oxidation. J Electrochem Soc 139(10):2736–2744
18. Gottrell M, Kirk DW (1993) A study of electrode passivation during aqueous phenol electrolysis. J Electrochem Soc 140(4):903–911
19. Lapuente R, Cases F, Garces P, Morallon E, Vazquez JL (1998) A voltammetric and FTIR-ATR study of tge electropolymerization of phenol on platinum electrodes in carbonate medium influence of sulphide. J Electroanal Chem 451(1-2):163–171
20. Iotov PI, Kalcheva SV (1998) Mechanistic approach to the oxidation of phenol at a platinum/gold electrode in acidic medium. J Electroanal Chem 442(1-2):19–26
21. Skowroński JM, Krawczyk P (2000) Electrochemical oxidation of phenol on exfoliated $HClO_4$-GIC and CrO_3-GIC in alkaline solution. Extended Abstracts in: 51th Annual Meeting of International Society of Electrochemistry, Warszawa, Poland Warsaw University: 2018
22. Matatov-Meytal YI, Sheintuch M, Shiter GE, Grader GS (1997) Optimal temperatures for catalytic regeneration of activated carbon. Carbon 35(10-11):1527–1531
23. San Miguel G, Lambert SD, Graham NJD (2001) The regeneration of field –spent granular activated carbons. Water Res 35(11):2740–2748
24. Valdes H, Zaror CA (2006) Ozonation of benzothiazole saturated-activated carbons: influence of carbon chemical surface properties. J Hazar Mat B137:1042–1048
25. Skowroński JM, Krawczyk P (2009) Enhanced electrochemical activity of regenerated expanded graphite electrode after exhaustion in the process of phenol oxidation. Chem Eng J 152(2-3):464–470
26. Krawczyk P, Rozmanowski T, Gurzęda B, Osińska M (2016) Process of phenol electrooxidation on the expanded graphite electrode accompanied by the in-situ anodic regeneration. J Electroanal Chem 775:228–234
27. De Heredia Beltran J, Dominguez JR, Lopez R (2004) Advanced oxidation of cork-processing wastewater using Fenton's reagent: kinetics and stoichiometry. J Chem Technol Biotechnol 79: 407–412, 4
28. Valdes H, Sanchez-Polo M, Rivera-Utrilla J, Zaror CA (2002) Effect of ozone treatment on surface properties of activated carbon. Langmuir 18(6):2111–2116
29. Krawczyk P (2011) Effects of ozone treatment on properties of expanded graphite. Chem Eng J 172(2-3):1096–1102
30. Wolborska A, Maryniak K, Perkowski J (2002) The effect of ozonation on sorption properties of active carbon and its porous structure. Model investigations. Pol J Chem Technol 4:42–46
31. Seredyńska-Sobecka B, Tomaszewska M (2007) The influence of ozonation on the activated carbon adsorption of phenol and humic acid. Pol J Chem Technol 9(4):107–110

32. Rivas FJ, Beltran FJ, Gimeno O, Frades J (2004) Wet air and extractive ozone regeneration of 4-chloro-2-methylophenoxycetic acid saturated activated carbons. Ind Eng Chem Res 43(15):4159–4165
33. Cabrera-Codony A, Georgi A, Gonzales-Olmos R, Valdes H, Martin MJ (2017) Zeolites as recyclable adsorbents/catalysts for biogas upgrading: removal of octamethylcyclotetrasiloxane. Chem Eng J 307:820–827
34. Peralta E, Roa G, Hernandez-Servin JA, Romero R, Balderas P, Natividad R (2004) Hydroxyl radicals quantification by UV spectrometry. Electrochim Acta 129:137–141
35. Świątkowski A, Grajek H, Pakuła M, Biniak S, Witkiewicz Z (2002) Voltammetric studies of the gradual thermal decomposition of activated carbon surface oxygen complexes. Colloids Surf A Physicochem Eng Asp 208(1-3):313–320
36. Świątkowski A, Pakuła M, Biniak A, Walczyk M (2004) Influence of the surface chemistry of modified activated carbon on its electrochemical behavior in the presence of lead (II) ions. Carbon 42(15):3057–3069
37. Laszlo K, Tombacz E, Josepovitz K (2001) Effect of activation on the surface chemistry of carbons from polimer precursors. Carbon 39(8):1217–1228
38. Park SJ (2002) Effect of KOH activation on the formation of oxygen structure in activated carbons synthesized from polymeric precursors. J Colloid Interface Sci 250(1):93–98
39. Terzyk AP (2001) The influence of activated carbon surface chemical decomposition on the adsorption of acetaminophen (paracetamol) in vitro: part II. TG, FTIR, and XPS analysis of carbons and the temperature dependence of adsorption kinetics at the neutral pH. Colloids Surf A Physicochem Eng Asp 177(1):23–45
40. Diaz-Teran J, Nevskaia DM, Fierro JLG, López-Peinado AJ, Jerez A (2003) Study of chemical activation of lignocellulosic material with KOH by XPS and XRD. Microporous Mesoporous Mat 60(1-3):173–181
41. Polovina M, Babić B, Kaluderović B, Dekanski A (1997) Surface characterization of oxidized activated carbon cloth. Carbon 35(8):1047–1052
42. Socrates G (2001) Infrared and Raman characteristic group frequencies. Tables and charts Wiley
43. Solum MS, Pugmire RJ, Jagtoyen M, Derbyshire F (1995) Evolution of carbon structure in chemically activated wood. Carbon 33(9):1247–1254
44. J. Zawadzki (1980) Spektroskopia w podczerwieni Zjawisk Powierzchniowych na Węglach, UMK, Toruń (in Polish)
45. Park SH, McClain S, Tian ZR, Suib SL, Karwacki C (1997) Surface and bulk measurements of metals deposited on activated carbon. Chem Mater 9(1):176–183